Multifunctional building parts
Increased solar shares with activated building parts

Tillman Gauer[1*], Matthias Pahn[1]
[1]Technische Universität Kaiserslautern, Kaiserslautern, Germany
***** *tillman.gauer@bauing.uni-kl.de*

Abstract

To achieve national and international climate goals, the greenhouse gas emissions from the building sector must be reduced. One option is the use of renewable energies, which must be stored. Building parts with thermal activation have the potential to store heat. As those building parts feature new active energetic functionalities – active heat storage and heating – they are called multifunctional building parts (MBP). To investigate the potential of MBP, a thermal model is deployed and verified. The model is used to examine the influence of the distance between thermal activation and the MBP's inside.

Introduction

To reach the climate goals of the building sector, e.g., a nearly climate-neutral building stock, the demand of buildings must be reduced by insulation and the residual heat demand must be covered carbon-free with renewable energies. One of those is solar heat. While it is ubiquitous, it cannot be controlled to meet demand. Thus, solar heat must be stored to cover the heat demand of a building. At current water-filled buffer storages are utilised. While covering small shares of the heat demand of a single-family dwelling with solar heat requires buffer storages of ab. 300 l, the required size increases disproportionately when covering 60 or even 80%. To avoid big buffer storages, heat can also be stored in any material, like external walls of single-family dwellings. To achieve the required change in temperature, the walls can be equipped with thermal activation. By connecting it to the heating system, solar heat can be transferred to the wall, which then is transferred to the adjacent room to cover the heating demand. As those building parts, in addition to their classic functionalities, like load-bearing, also fulfil the active thermal functions of storage and heating, they are called multifunctional building parts (MBP). Figure 1 shows a lying cross-section of such an MBP as an extern wall. Producing it as a precast concrete element brings several advantages, like higher quality and faster installation on the construction site. In addition, MBP can also be more easily integrated into buildings that are not made of concrete – precast elements or in-situ concrete.

Figure 1: (Lying) cross-section of a multifunctional building part designed as an external wall.

To show the potential of the MBPs, a single-family dwelling, according to IEA SHC Task32, was equipped with a solar thermal collector of 40 m² and an electric heat pump, see (Heimrath and Haller 2007). By utilising the Northern façade as MBPs, the demand for electric energy was reduced by up to 40%. Further information can be found in (Gauer and Pahn 2022).

A model was developed in MatLab to investigate the MBP further and needs to be verified with measurement data from the full-scale demonstrator 'SmallHouse IV'. Based on the developed model, the influence of the position of the thermal activation is investigated.

Methods

The model used for the MBP is based on the model developed by Javanmardi and published in (Javanmardi et al. 2017). This verification was done using a small-scale specimen and under defined boundary conditions in a laboratory. Filling the lack of a verified full-scale demonstrator under real conditions is done in two steps. In the first step, the building is let cool down while exposed to cold weather. In the second step, the external wall of the full-scale demonstrator 'SmallHouse IV' is tested by heating up the MBP at a constant flow temperature and letting it cool down. Further and up-to-date information on the 'SmallHouse IV' can be found online (Gauer).

The active layer's position is investigated by coupling the verified model of the MBP with a model for the building envelope and the heating system using TrnSys 17.

Demonstrator building 'SmallHouse IV'

A full-scale demonstrator was built at the Technische Universität Kaiserslautern to validate these results and the models, see figure 2. All walls of this 8 x 5-meter single-room building are precast concrete elements utilised as MBP. Alike the representative model, it features a solar thermal collector and an electric heat pump, see figure 3. It aims to emulate a single-family dwelling; therefore, the surface is relatively high compared to the encapsulated volume.

Figure 2: Full-scale demonstrator 'SmallHouse IV' from the southwest made of multifunctional building parts, incl. two exchangeable elements and the solar thermal collector.

The 'SmallHouse IV' is equipped with a solar thermal collector of 15 m² apparatus area facing south. The collector can feed the heat into the MBP, a buffer of 500 l or a ground storage of 5 x 8 x 1.4 m below the building. By using this priority, the MBPs are used primarily. Further details on the control can be found at (Gauer and Pahn 2019). A ground heat pump guarantees sufficient heat supply at all times. The heat pump takes heat from the ground storage and thus can make use of solar heat. By introducing horizontal insulation stretching into a depth of 1.4 m from the surface, the losses to the ambient ground can be reduced. The insulation also reduces the mass flow of groundwater below the building. The MBPs, forming all the external walls, primarily cover the heating demand by forwarding the heat to the adjacent room. The residual heating demand is covered by the floor heating, which is fed from the buffer storage, see figure 3.

Further information on the design, concept and production of the 'SmallHouse IV' can be found in (Pahn et al. 2019). In comparison, fundamental studies on the design of the MFB and the evaluation of their thermal can be found in (Caspari et al. 2015).

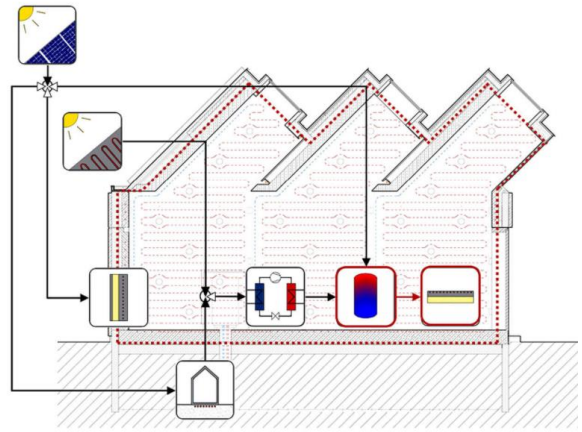

Figure 3: Full-scale demonstrator 'SmallHouse IV' from the southwest made of multifunctional building parts, incl. two exchangeable elements and the solar thermal collector.

Multifunctional building part

The above described and depicted building parts are used to verify the MatLab model of the MBP. The used cross-section consists of a load-bearing layer with a thickness of 21 cm, an insulation layer of 14 cm, and a facing shell of 7 cm. While the insulation has a thermal conductivity of $\lambda = 0.04$ W/(m.K), the other layers are made of standard concrete ($\lambda = 2.1$ W/(m.K); $c_p = 2{,}400$ kg/m³), see figure 4.

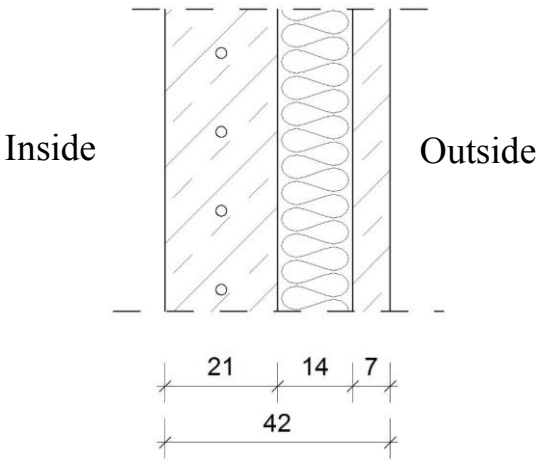

Figure 4: Cross-section of the MBP of the 'SmallHouse IV' used for the verification, with load-bearing, insulation, and facing shell (from left to right).

The temperatures of the load-bearing layer are monitored at the core and 3 cm off the inner and outer surface.

Simulation parameters and indicators

The thermal behaviour of the MBP is influenced by the thermal resistance between the active layer and the inside of the building. This resistance can be changed by the activation's position and the activated layer's thermal conductivity. Likewise, the thermal capacity of the load-

bearing layer influences the thermal behaviour of the MBP. In the following, the impact of the parameters is investigated according to table 1. The impact is measured by the heat generated and consumed and the electric demand.

Table 1: Parameters of the activated layer of the MBP being investigated.

NAME	LOW	AV.	HIGH
Distance between the activation and the inner surface of the MBP [cm]	4.5	10.5	16.5
Thermal conductivity [W/(m.K)]	1.8	2.1	2.4
Thermal capacity [kJ/(kg.K)]	0.5	1.0	2.0

The 3 resulting variants are being compared using the energy production and consumption of the whole year, see table 2. Along with those, representative excerpts of the temperature of the MBP are being observed. The room air temperature is used as an indicator of thermal behaviour.

Table 2: Indicators.

NAME	ABBREVIATION
Solar thermal generation	(Q_{ST})
Heat generation heat pump	(Q_{HP})
Heat delivered to MBP	(Q_{MBP})
Electric energy demand of the heat pump	(W_{HP})
Total electric energy demand	(W_{tot})

Model verification – Building envelope

To verify the model of the building envelope of the 'SmallHouse IV', see figure 6, the demonstrator was heated to a room air temperature of 24°C and then let cool down for 6 days (Jan 24th 2020, to Jan 29th 2020). The outer temperature was between -2 and 4°C, so at a relatively constant level. The room air temperature was used for the comparison, as indicated in figure 5. The results show a good comparison between the measured and the simulated data, as an R^2-value of 0.968 indicates. Therefore the model of the building envelope can be considered verified. The characteristic peaks of the temperature curve result from the solar gains onto the building around noon each day.

It was found that the initial thermal properties of the MBP, derived from the blueprints, resulted in good comparisons. More adjustments were necessary to account for the thermal load of about 200 W, resulting from electronic devices for measurement and control of the demonstrator.

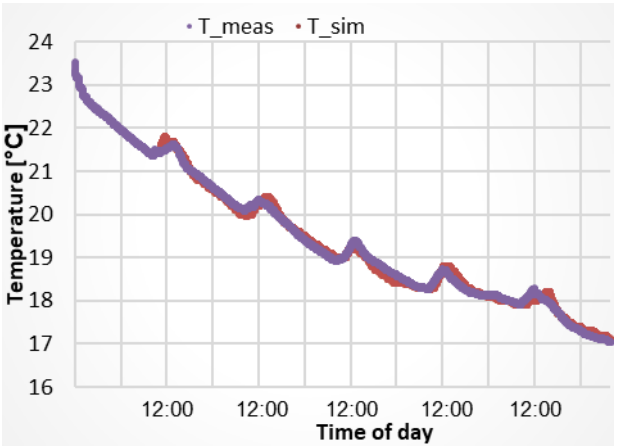

Figure 5: Measured and simulated room air temperature during the cool-down period.

Model Verification – Building part

Alike the whole building envelope, the model for the MBP needs to be verified. The therefore required

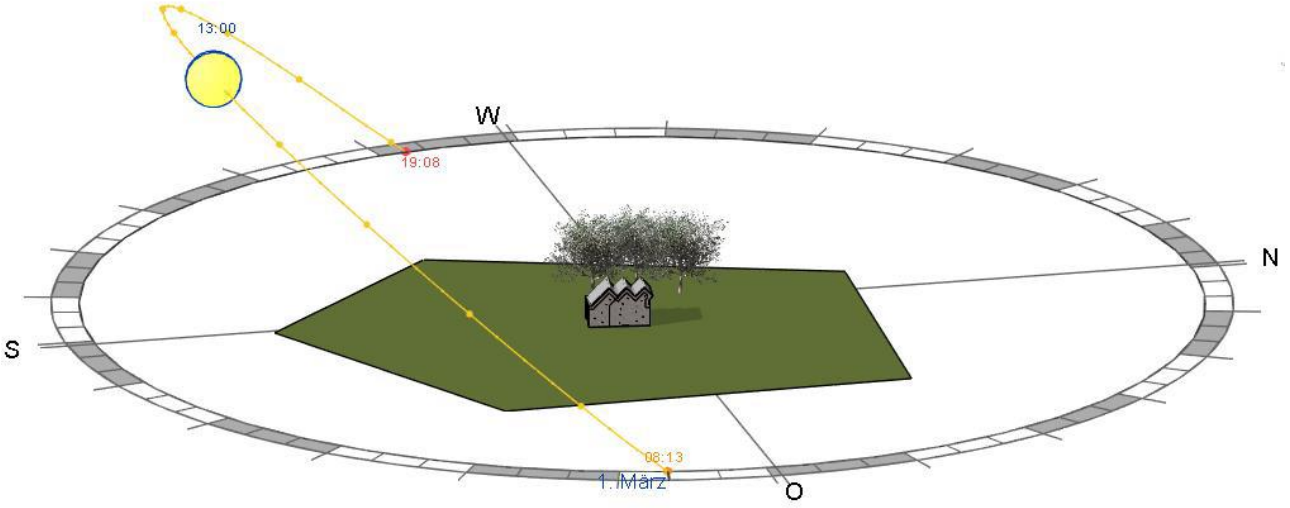

Figure 6: Modell of the 'SmallHouse IV' for the thermal simulation

measurement data is gathered by heating the described MBP with a constant flow temperature of T_{flow} = 50°C for about 5 h. Figure 5 shows the temperature of the three sensors – inner (blue), core (red) and outer (green) - distribution over time. The start of the mass flow of the active layer can be seen clearly after about 2 h. Furthermore, the nearly simultaneous increase of the outer and the inner temperature can be observed. Besides a steeper incline within the first hour, a rate of temperature change of 1 K/h is evitable. This behaviour can be drawn back to the fact that the load-bearing layer is at a constant temperature of T_{start} = 24.5°C and the outer insulation reduces thermal losses significantly.

In contrast, the core temperature increases significantly erratic by 4 K within about 15 minutes. After this, a nearly continuous increase can be observed with a rate of 0.88 K/h. This jump in temperature results from the short distance between the thermal activation and the temperature sensor of the core layer.

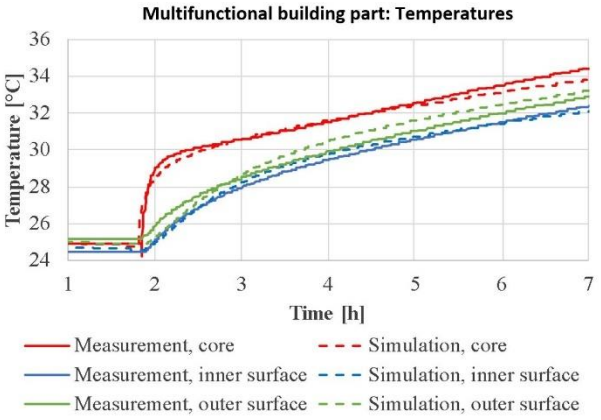

Figure 7: Comparison of the measured and simulated temperatures in the MBP.

Compared to the simulation data indicated with dashed lines, good accordance can be found. The differences are below 0.4 K at all times. While the core and the inner show the discrepancies, the outer diverges most.

When investigating all sensors, a coefficient of determination of R^2 = 0.974 can be found, indicating good accordance between the measured and the simulated temperature data. Therefore, the model can be approved for further simulation.

Simulation results

The verified models are then used to investigate the influence of the distance between the active layer and the inner surface on the thermal behaviour of the heating system.

Energy balances

The annual heat generation is indicated in figure 8. The solar gains accumulate to 4,180 to 4,280 kWh_{th}/a, increasing with increasing distances of the activation from the inner surface, see figure 8. From this, shares of the heat pump to 15% to 16% result.

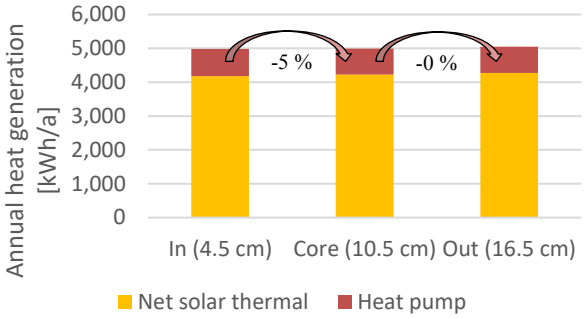

Figure 8: Heat generation with respect to the position of the activation.

The heat transferred to the MBP or the floor heating covers the heating demand. Figure 9 shows that about 3,390 to 3,525 kWh_{th}/a are transferred to the MBP, again increasing with increasing distance from the inner surface. The floor heating is nearly constant in all variants at 1,470 kWh_{th}/a. Analogous, the MBP accounts for 70% of the heat consumed.

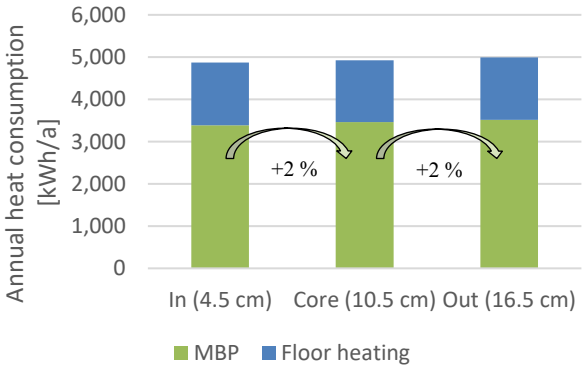

Figure 9: Heat generation depending on the position of the activation.

Figure 10 shows the demand for electric energy for heat production. It can be seen that the demand for electric energy is nearly constant at 630 kWh_{el}/a.

Furthermore, it shows that the heat pump accounts for 66% of all cases investigated. When compared with the heat generated, a clear flip can be observed. This is because the heat production of the solar thermal collector is much more efficient when compared to the one of the heat pump. While the first has a seasonal COP of about 32 to 39. The heat pump's seasonal efficiency is 6.9 for the outer, 7.0 for the inner position and 7.7 for the core position. The difference results from the heat used by the floor heating indicated above. The heat pump's efficiency is increased as the core position leads to a more efficient use of solar heat, which leads to a lower share of the heat

pump during times with low solar radiation, which results in reduced efficiency.

From this, it must be concluded that the influence of the position of the thermal activation has only a neglectable impact on the overall performance of the building.

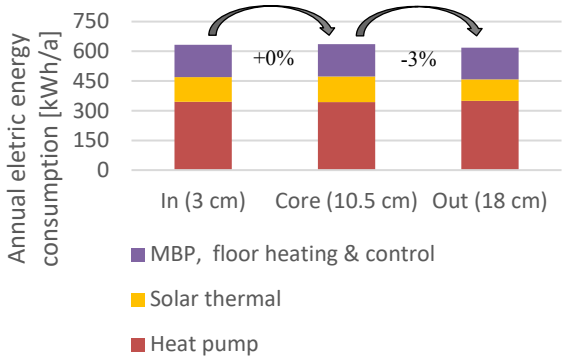

Figure 10: Demand for electric energy with respect to the activation position.

As figure 11 shows, the thermal capacity of the activated layer influences heat generation. The solar generation increases slightly from 4,175 to 4,275 kWh_{th}/a or about 2%. Likewise, the heat pump's heat generation increases with an increased capacity from 1,325 to 1,775 kWhth/a or by about 25%.

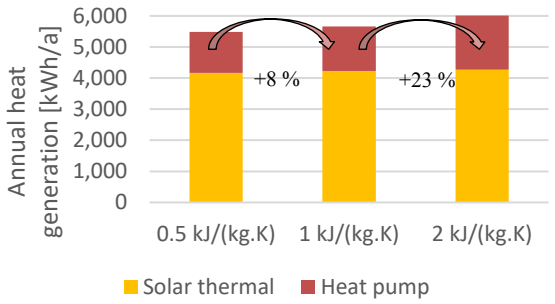

Figure 11: Heat generation with respect to the thermal capacity of the load-bearing layer.

Like heat generation, heat consumption is influenced by the thermal capacity of the activated load-bearing layer, as indicated in figure 12. The heat transferred to the MBP increases from 3,275 to 3,575 kWh_{th}/a or by about 8% with increasing capacity. In contrast, the floor heating's consumption is nearly identical to the low and the average capacity at 1,450 kWh_{th}/a but increases to 1,725 kWh_{th}/a or by 16% when increasing the heat capacity.

This behaviour must be interpreted that more solar heat is being stored in the MBP with increasing capacity. Still, the additional heat does not contribute to the covering of the heating demand.

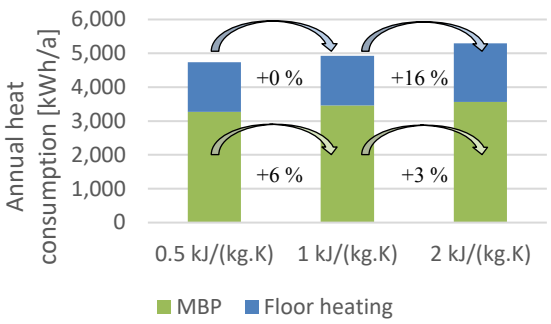

Figure 12: Heat generation with respect to the thermal capacity of the load-bearing layer y.

Alike in the other cases investigated, the heat pump has the biggest demand for electric energy, see figure 13. Nevertheless, the total annual demand for electric energy is nearly identical for all variants at 635 kWh_{el}/a. Only using a high capacity results in a about 1.5% increased demand of 645 kWh_{el}/a. This increase can be drawn back to the increased demand of the heat pump. As described, this results from the solar heat being stored in the MBP but does not contribute to cover the heating demand.

From this, it must be concluded that the thermal capacity of the activated layer has only a tiny impact on the system's overall performance. Nevertheless, lower capacities are preferable to higher ones. This effect may result from the fact that when loading the same amount of heat to the MBP, the temperature of the MBP decreases with an increased thermal capacity. This results in a lower temperature difference to the inner, leading to a lower heat transfer and a longer duration of heat storage.

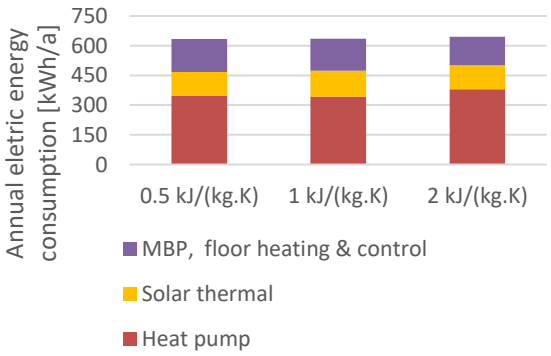

Figure 13: Demand for electric energy with respect to the thermal capacity of the load-bearing layer.

The impact of the thermal conductivity of the load-bearing layer on the heat generation is shown in figure 14. Unlike the other parameters, no significant difference can be observed, as the solar collector contributes about 4,250 kWh_{th}/a and the heat pump 1,450 kWh_{th}/a in all cases investigated.

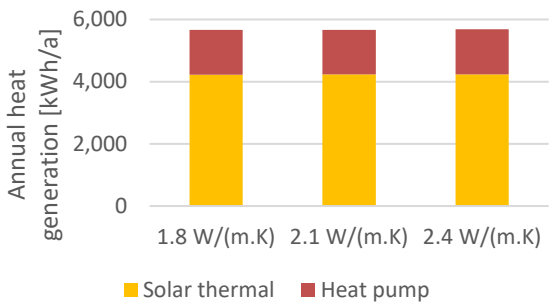

Figure 14: Heat generation with respect to the thermal conductivity of the load-bearing layer.

Also, the heat consumptions of the floor heating and the MBP are nearly constant at 1,470 kWh_{th}/a or 3,460 kWh_{th}/a, respectively.

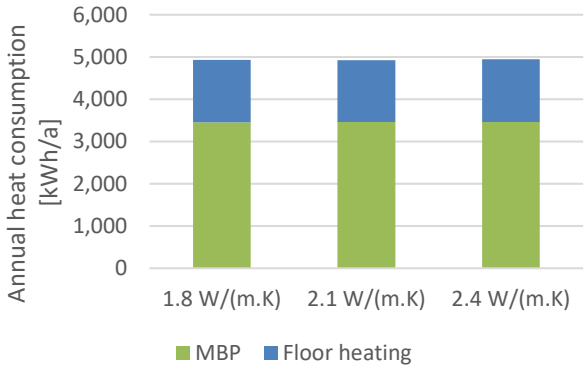

Figure 15: Heat consumption with respect to the thermal conductivity of the load-bearing layer.

Unlike the thermal indicators, the total annual electric demand decreases with an increasing thermal conductivity from 654 to 623 kWh_{el}/a or by 5%. This reduction can be deducted from the heat pump. Its efficiency increases from 4.0 to 4.2 with increasing thermal conductivity.

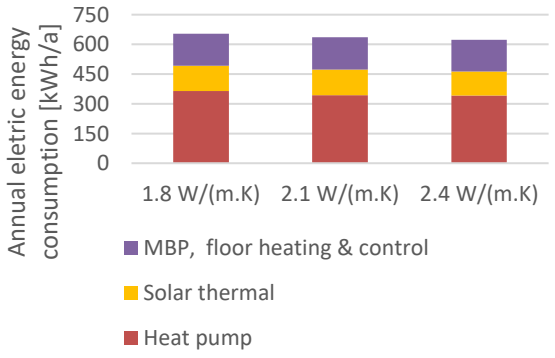

Figure 16: Demand for electric energy with respect to the thermal conductivity of the load-bearing layer.

It can be concluded that the thermal conductivity of the activated layer – in the scope investigated – impacts the overall electric demand. This influence results from faster heat shifts and lower temperatures in both storages. The reduced temperature of the buffer storage then leads to increased efficiency and ultimately a reduced electric demand of the heat pump.

Discussion

The simulation results indicate that the use of normal concrete leads to the desired heat storage and desired reduction of electric energy. The simulation results furthermore show that the change of individual thermal properties of the concrete does not lead to any significant changes. Similar results can be found regarding the position of the thermal activation.

Conclusion

Good accordance for the two models used was found. Therefore, the models are approved and may be used for further investigations.

The 2 thermal properties of the activated layer, like the position of the activation, show only a neglectable impact on the overall performance of the MBP. This performance is measured using the total annual electric demand, which is the base for further investigations like GHG emissions or annual costs for heating.

The low impacts of the thermal properties can be interpreted so that no additional requirements result from utilising a building part as an MBP. The same applies to the position of the thermal activation. Both findings might lead to a better economic performance of MBP.

The used and presented full-scale demonstrator 'SmallHouse IV' – as a real building and a thermal model – bears the potential to investigate further the properties of MBP and the usage of new materials, like phase-change material (PCM) or switchable insulations. Especially the thermal model allows for investigation of the control of heating systems with MBP and their potentials, e.g. for sectoral coupling.

Acknowledgements

The authors like to thank all supporters. This support includes not exhaustively but in particular funding by the German Ministry for Interior and the state of Rhineland-Palatinate along with the European Union.

Nomenclature

COP: Coefficient of performance

GHG: Greenhouse gas

HP: Heat pump

MBP: Multifunctional building part

ST: Solar thermal or solar thermal collector

References

Caspari, C., Krumke, S. O., Pahn, M. (2015) Entwicklung multifunktionaler Bauteile mit Hilfe mathematischer Optimierungsmethoden, in: Kornardt, O., Hoffmann, S., Lorenz, D., Pahn, M. and Völker, C. (Eds.). *Tagungsband der Bauphysiktage Kaiserslautern 2015:* Schriftenreihe des Fachgebiets Bauphysik/Energetische Gebäudeoptimierung, Eigenverlag, pp. 103–106

Gauer, T. SmallHouse IV online [online] https://mb-web.bauing.uni-kl.de/smallhouse

Gauer, T., Pahn, M. (2019) Multifunctional components for the active energetic use of the building envelope, in: Advanced Building Skins GmbH (Ed.). *14th Conference on Advanced Building Skins, 28-29 October 2019, Bern, Switzerland*, Advanced Building Skins GmbH, Lucerne (Switzerland), pp. 715–725

Gauer, T., Pahn, M. (2022). Multifunctional building parts to increase the use of solar thermal heat in residential buildings – Mechanisms, saving potentials and application under real conditions, *Journal of Building Engineering* 51, 104278, DOI: 10.1016/j.jobe.2022.104278

Heimrath, R., Haller, M. (2007) The Reference Heating System, the Template Solar System of Task 32: A Report of IEA Solar Heating and Cooling programme - Task 32 "Advanced storage concepts for solar and low energy buildings". Graz

Javanmardi, R., Bavani, A. M., Pahn, M. (2017) Numerische Lösung des thermischen Verhaltens von Bauteilen mit PCM- und thermisch aktivierten Schichten, in: Kornadt, O. (Ed.). *Bauphysiktage Kaiserslautern 2017:* Bauphysik in Forschung und Praxis, Eigenverlag, Kaiserslautern, pp. 57–59

Pahn, M., Bayer, D., Krumke, S. O., Caspari, C., Gauer, T., Schluppkotten, D. M., Holzhauser, M., Weiler, T. (2019) Großdemonstrator - multifunktionale Betonfertigteile für energetisch nutzbare Gebäudetragstrukturen. Fraunhofer IRB Verlag, Stuttgart